

# ANALYSIS OF THE EVOLUTION OF SPACE DEBRIS THROUGH A SYNTHETIC POPULATION

Daniel Casanova\*, Anne Lemaitre<sup>†</sup> and Alexis Petit<sup>‡</sup>

Space debris are all man-made objects orbiting the Earth which no longer serve a useful function. Space debris have increased substantially in the last decades and can be counted in millions. This paper deals with the idea of the creation of a synthetic population of space debris, which preserves as accurate as possible the characteristics of the real one. All the individuals of the synthetic population will be propagated by powerful numerical integrators, becoming into an excellent tool for global predictions or simulations, useful for the future ADR actions, and for the location of parking orbits.

## INTRODUCTION

Space debris are all man-made objects of all sizes and all chemical compositions orbiting the Earth which no longer serve a useful purpose. The number of space debris objects has substantially increased in the last decades becoming into a real problem for the space missions since continuous avoidance maneuvers are performed, by the active satellites, the space shuttles or the ISS to avoid the risk of collision with the biggest objects, increasing the cost of the missions.

This paper deals with the idea of the creation of a synthetic (artificial) population of space debris. This synthetic population represents the real one, and preserves its characteristics. The strength of the idea consists of the predictions that can be done through the numerical computation of the orbits of each piece of space debris that compound the synthetic population.

Similar works are based on the creation of a synthetic population of millions of persons to simulate and understand the daily travels, flows and traffic jams, in the whole country of Belgium.<sup>1,2</sup> The idea consists of applying similar techniques to built the synthetic population of space debris. In this particular problem, we have real data coming from the TLE catalog (the largest objects), different catastrophic events (such as the collision between Cosmos 2251 and Iridium 33, or the intentional explosion of the Fengyung 1C),<sup>3</sup> surveys or simulations, at different times, at different locations obtained by different methods.

The synthetic population will contain the objects from the TLE catalog but also a large number of objects with a great diversity in their area-to-mass ratio, which is a variable that plays a crucial role in their orbit evolution. The building of our synthetic population will use a Synthetic Reconstruction (SR) method, which consists of generating the synthetic population by using a real sample of space debris population and an Iterative Proportional Fitting Procedure (IPFP).<sup>4</sup> Thus, we would obtain a synthetic population of space debris which approximates as well as possible the real one.

---

\*Profesor Ayudante Doctor, Centro Universitario de la Defensa - Zaragoza and IUMA - Universidad de Zaragoza (Spain)

<sup>†</sup>Professor, Department of Mathematics, University of Namur, Namur (Belgium)

<sup>‡</sup>PhD, Department of Mathematics, University of Namur, Namur (Belgium)

Once the synthetic population is built, we use powerful and already implemented tools to analyze the time evolution of the population. We use a powerful numerical integrator, named NIMASTEP,<sup>5</sup> to compute the short and long term evolution of each piece of space debris that compound the synthetic population. We use different analytical models to better understand the evolution of the population, and a three-filter sequence to avoid and detect possible collisions between two objects of space debris orbiting the Earth. At this point, it will be possible to extract global properties of the synthetic population such as dispersion, stability and concentration. The obtained results will coincide with the properties of the real population. Then, the synthetic population becomes into a powerful method for global predictions or simulation of space debris.

The paper is organized as follows. First, we describe the current situation of space debris. Then, we present different tools that have been already developed for the analysis of the evolution of space debris. After that, we show two different techniques to compute a synthetic population of space debris, and finally we analyze how the synthetic population will contribute to global predictions.

## **SPACE DEBRIS CURRENT SITUATION**

Since the launch of Sputnik I in 1957 by the Soviet Union, more than 7000 satellites have been launched into space generating a huge amount of space debris. Currently, the space debris situation has become into a real problem for the new space missions and it seems to get worse in the near future. Figure 1 illustrates the increase in space debris during the last few years, and it can be guessed the future exponential growth of space debris that will become into an even more dangerous situation. We have different tools to obtain information of the existing pieces of space debris. For example, the Two Line Elements (TLE) catalog contains the information concerning the location of about 40,000 objects including active, non-active satellites, and objects larger than 10 cm. However, the number of space objects smaller than 10 cm in size can be counted in millions. This means that the TLE catalog represents the tip of the iceberg. The smallest debris are much more numerous, with rough estimations of about 200,000 objects between 1 and 10 cm and more than 35 millions of objects between 0.1 and 1 cm. These debris are neither cataloged nor individually identified. For this reason, special equipment and armor plating protection are now systematically scheduled for the spacecraft, increasing their cost and requiring even more powerful rockets. Furthermore, continuous avoidance maneuvers are performed, by the active satellites, the space shuttles or the ISS to avoid the real risk of collision with the biggest objects, increasing the cost of the missions by fuel consuming.

## **TOOLS FOR THE ANALYSIS OF SPACE DEBRIS EVOLUTION**

The current situation described above requires new methodologies to study the evolution of the space debris population. To overcome this problem we first develop different tools to analyze the evolution of a piece of space debris. In particular, analytical models are developed to better understand the time evolution of a piece of space debris. Numerical methods are also developed to predict precisely the orbit evolution. Finally, a method to detect collisions between pieces of space debris has been implemented. In this section, we briefly describe the mentioned tools.

### **Analytical Model**

The development of analytical methods to describe the orbit evolution of space debris are mainly interesting for two reasons. One reason is that they allow a better understanding of the problem since it is possible to know the effect of the different perturbations on the long-periodic motion, the

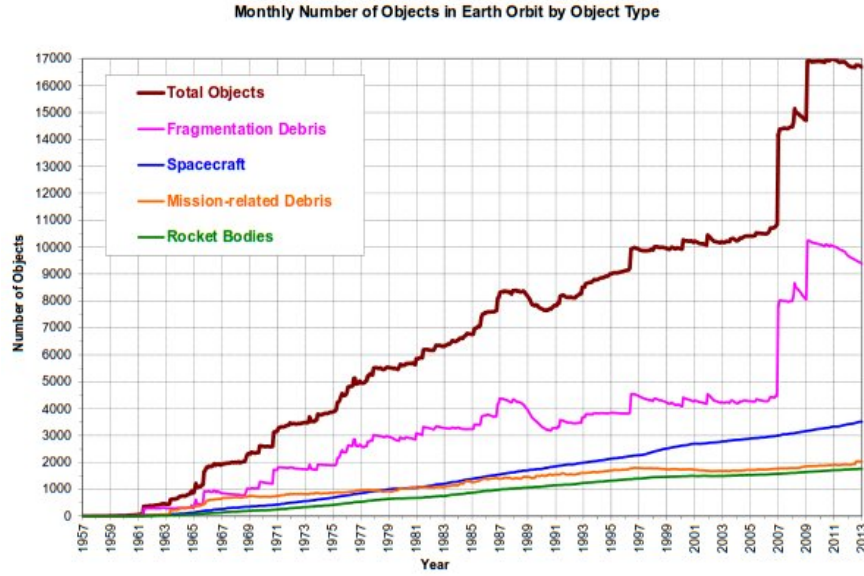


**Figure 1. Growth of debris (in the TLE catalogue) from 1957 to 2013 (Source: NASA)**

amplitude of the oscillatory motion, etc. The other reason is that the computation of the position of a piece of space debris object in its orbit is faster when an analytical expression is available.

The naXys team, from the University of Namur, has developed different analytical methods to compute the orbit evolution of an object orbiting a rigid body. The proposed models take into account the attraction of the Earth as a point mass central body, the effect of the solar radiation pressure,<sup>6</sup> the inclusion of the Earth gravity field, particularly the  $J_2$  effect,<sup>7</sup> and the inclusion of the Sun as a third body.<sup>8</sup>

The analytical model uses the following autonomous Hamiltonian function:

$$\mathcal{H}(\vec{r}, \vec{v}) = \mathcal{H}_K(\vec{r}, \vec{v}) + \mathcal{H}_{geo}(\vec{r}) + \mathcal{H}_{SRP}(\vec{r}) + \mathcal{H}_{\odot}(\vec{r}), \quad (1)$$

where  $\vec{r} = (x, y, z)$  and  $\vec{v} = (\dot{x}, \dot{y}, \dot{z})$  represent the position and velocity vector of the piece of space debris in a fixed inertial equatorial geocentric frame. The model takes into account the attraction of the Earth as a point mass central body ( $\mathcal{H}_K(\vec{r}, \vec{v})$ ), the perturbations due to the  $J_2$  effect ( $\mathcal{H}_{J_2}(\vec{r})$ ), the solar radiation pressure ( $\mathcal{H}_{SRP}(\vec{r})$ ) and the effect of the Sun as third body ( $\mathcal{H}_{\odot}(\vec{r})$ ).

To describe the motion of an object around a rigid body the classical orbital elements are used. However, when the eccentricity approaches zero the argument of perigee is not defined, and a similar situation happens when the inclination is close to zero. To overcome this problem the proposed model uses canonical and non-singular variables, named Poincaré's variables:

$$\begin{aligned} x_1 &= \sqrt{2P} \sin p, & y_1 &= \sqrt{2P} \cos p, \\ x_2 &= \sqrt{2Q} \sin q, & y_2 &= \sqrt{2Q} \cos q, \\ \sigma &= \lambda - \theta, & L &, \end{aligned} \quad (2)$$

where  $\lambda$  is the mean longitude, which is the sum of the mean anomaly, argument of perigee, and the longitude of the ascending node. The variable  $\theta$  is the sidereal time and  $L$  is one of the classical

Delaunay's elements given by:

$$L = \sqrt{\mu a}, \quad G = \sqrt{\mu a(1 - e^2)}, \quad H = \sqrt{\mu a(1 - e^2)} \cos i.$$

Finally, the modified Delaunay's elements are defined by:

$$\begin{aligned} P &= L - G, & p &= -\omega - \Omega, \\ Q &= G - H, & q &= -\Omega. \end{aligned} \tag{3}$$

By using this model, it is possible to obtain an analytical expression to compute the position of a piece of space debris at a given time.<sup>8</sup>

### Numerical Integrator

An analytical solution allows a better understanding of the problem but it has limitations, and consequently, a numerical approach is required to determine an accurate solution of the problem. The numerical integrator NIMASTEP<sup>5</sup> takes into account the following forces acting on a piece of space debris; the non-spherical shape of the central body, the solar radiation pressure, the third body attraction, and it is possible to include a thrust acceleration. NIMASTEP also includes other useful tools to know global properties of an object orbiting a rigid body such as the MEGNO chaos indicator or the Frequency Map Analysis. However, this old version neglects the effect of the atmospheric drag.

Currently, the old version of NIMASTEP is being improved by including the effect of the atmospheric drag through the new model, Jacchia-Bowman 2006,<sup>9</sup> and making the software parallelizable, becoming into a more accurate and faster numerical integrator. The atmospheric drag cannot be neglected for space debris in Low Earth Orbits since it is one of the main perturbations that affects space debris evolution. Finally, by applying some parallelization techniques it is possible to compute the evolution of hundreds of pieces of space debris at the same time making the propagation of the population a faster process.

### Collision Avoidance and Detection

Another implemented tool consists of a new method to detect space debris collisions. The collision between two pieces of space debris or between a piece of space debris and an operative satellite is a real problem. We use the numerical integrator NIMASTEP to compute the orbit evolution of each piece of space debris, then we search for a time of coincidence in their orbit evolution. For that purpose we need to compare the orbit evolution of each pair of space debris. An all in all comparison is unfeasible by the enormous time consuming of the process, and consequently, a three-filter sequence is proposed.<sup>10,11</sup>

The method consists of reducing the possible pairs of candidates for a collision into a short list of pairs that are at real risk of collision through a three-filter sequence. *Filter I* is based on the computation of the geocentric distance  $\vec{r}(t)$  and its time derivative  $\dot{\vec{r}}(t)$  at any instant of time  $t$  of a piece of space debris. So, given a pair of objects of index  $s_1, s_2$ , we compute the maximum and minimum values of their geocentric distances, named  $\max(r_{s_j}), \min(r_{s_j})$ , for  $j = 1, 2$ . Then, we set  $q := \max\{\min(r_{s_1}), \min(r_{s_2})\}$  and  $Q := \min\{\max(r_{s_1}), \max(r_{s_2})\}$ . If the condition  $|q - Q| > D$ , with  $D$  a fixed threshold distance, holds, then there is no possibility for an orbit crossing and the selected couple is rejected. *Filter II* computes the orbit distance with sign at any

instant of time for each pair of objects. If there is a change of sign in this distance function an orbit crossing occurs. This filter is based on the Minimum Orbital Intersection Distance (MOID) concept. *Filter III*, also named time filter, computes the position of the two pieces of space debris looking for a time of coincidence. If there is an instant of time where the distance between the two pieces is smaller than a threshold distance  $D$ , the pair is considered at real risk of collision, otherwise the couple is disregarded.

## SYNTHETIC POPULATION

The synthetic population of space debris will be created by using space debris data coming from existing sources such as the Two Line Elements catalog, different catastrophic events, radar observations, etc. We will generate new space debris by using the characteristics of the known data.

### Real Data

Each piece of space debris has different characteristics that we gather into the attribute vector, given by:

$$\vec{v} = (a, e, i, \Omega, \omega, M, \beta^*)$$

where  $a$  is the semi-major axis,  $e$  is the eccentricity,  $i$  is the inclination,  $\Omega$  is the longitude of the ascending node,  $\omega$  is the argument of perigee,  $M$  is the mean anomaly, and  $\beta^*$ , named BSTAR, represents the radiation pressure coefficient.

The BSTAR parameter is measured in Earth radii<sup>-1</sup> and is given by:

$$\beta^* = B \frac{\rho_0}{2},$$

where  $B$  is the ballistic coefficient and  $\rho_0$  is the reference value of atmospheric density. The ballistic coefficient, named B-Term, represents how susceptible an object is to drag (the higher the value, the more susceptible). This term is the drag coefficient  $C_d$  multiplied by the area-to-mass ratio ( $A/m$ ) of the object,

$$B = C_d \frac{A}{m}.$$

The BSTAR coefficient is directly proportional to the  $A/m$  ratio of the piece of space debris, meaning that, the bigger the ratio  $A/m$  is, the bigger the BSTAR coefficient is, and vice versa.

### Creation of the Synthetic Population

The creation of the synthetic population is based on the work of Beckman et al.<sup>12</sup> by the construction of multiway tables, which relate the components of the attribute vector between each other. Then, if we know the total number of members in the population it is possible to construct the synthetic population with an Iterative Proportional Fitting Procedure (IPFP) and a Synthetic Reconstruction (SR) technique. This method will be applied with an estimated number of space debris objects to design a complete synthetic population of space debris.

As a first approach to the future implementation of the previously mentioned technique to build a synthetic population, we consider the marginal distribution of each component of the attribute vector and we built a synthetic population following two different techniques:

*First Technique:* Given  $n$  pieces of space debris we create a new population compound of  $2n$  pieces. The new population is composed of the  $n$  known objects plus  $n$  artificial objects, whose attribute vector is created according to the marginal distribution of each component of the attribute vector of the known population. The procedure is as follows:

1. We consider an initial population of  $n$  pieces of space debris taken from the TLE catalog.
2. We study the marginal distribution of each component of the attribute vector. We create  $n$  new pieces of space debris whose attribute vector has similar characteristics as the ones of the known population. For example, we consider the semi-major axis of the  $n$  pieces of space debris taken from the TLE and we study the marginal distribution of this attribute. Then, the new  $n$  pieces of space debris will have a semi-major with similar marginal distribution as the known population. We proceed in a similar way for each component of the attribute vector.

*Second Technique:* Given  $n$  pieces of space debris we create a new population compound of  $2n$  pieces. The new population is composed of, as in the previous technique, the  $n$  known objects plus  $n$  artificial objects, whose attribute vector is created according to the marginal distribution of each component of the attribute vector of the known population, except for the BSTAR coefficient. The procedure is as follows:

1. We consider an initial population of  $n$  pieces of space debris taken from the TLE catalog.
2. We proceed as in the *first Technique*, except for the BSTAR coefficient. In this technique the new objects will have a completely different BSTAR coefficient. Thus, the new pieces of space debris will be located in similar orbits, but they will have different  $A/m$  ratio.

## **SYNTHETIC POPULATION EXAMPLE**

In this section we apply the above mentioned two different procedures to create a synthetic population of space debris. Then, we analyze the evolution of the cloud of space debris.

### **Synthetic Population Created by the First Technique**

If we consider the 2653 objects, taken from the TLE catalog, that compound the cloud of space debris corresponding to the FENGYUN 1C catastrophic event, it is possible to obtain the marginal distribution of all the components of the attribute vector, i.e. the semi-major axis, the eccentricity, etc.

In the case of the semi-major axis, all the objects of the cloud are expected to have a different value since we are dealing with real numbers. For this reason, we propose to analyze the number of objects that have the semi-major axis within a specific range. Table 1 catalogs the number of objects in the cloud within ten different ranges. Remark that, depending on the number of objects in the population the discretization of the semi-major axis can be more rigorous.

We obtain similar tables for each element of the attribute vector. In particular, Table 2 catalogs the objects of the cloud of space debris depending on its BSTAR coefficient. A rigorous analysis of the marginal distribution of the  $\beta^*$  coefficient is required since the majority of these space debris objects have a small BSTAR coefficient, which means that the ratio  $A/m$  is quite small. Figure 2 shows the BSTAR coefficient of each piece of space debris that compound the cloud of FENGYUN 1C.

**Table 1. Frequencies of the semi-major axis (a) for the FENGYUN 1C cloud of space debris**

a [km]	Objects	a [km]	Objects
$a < 6,500$	0	$6,500 < a < 7,000$	87
$7,000 < a < 7,100$	255	$7,100 < a < 7,200$	615
$7,200 < a < 7,300$	1190	$7,300 < a < 7,400$	312
$7,400 < a < 7,500$	129	$7,500 < a < 8,000$	58
$8,500 < a < 9,000$	6	$a > 9,000$	1

**Table 2. Frequencies of the BSTAR coefficient for the FENGYUN 1C cloud of space debris**

BSTAR [ $r_{\oplus}^{-1}$ ]	Objects	BSTAR [ $r_{\oplus}^{-1}$ ]	Objects
$\beta^* < 0.0$	9	$0.0 < \beta^* < 0.0005$	463
$0.0005 < \beta^* < 0.001$	395	$0.001 < \beta^* < 0.0015$	293
$0.0015 < \beta^* < 0.002$	251	$0.002 < \beta^* < 0.003$	515
$0.003 < \beta^* < 0.004$	317	$0.004 < \beta^* < 0.005$	148
$0.005 < \beta^* < 0.01$	214	$\beta^* > 0.01$	48

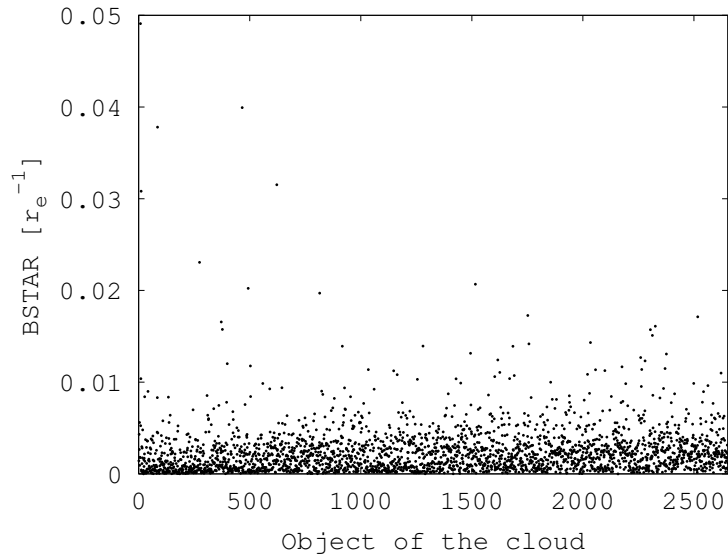


**Figure 2. The BSTAR coefficient for each of the elements of the cloud of FENGYUN 1C**

Once the marginal distribution of the objects of the cloud of space debris has been studied, it is possible to create the new population compound of double elements i.e. 5306 pieces of space debris. To clarify how the attribute vectors are generated we explain the particular case of the semi-major axes. The initial population has 87 objects whose semi-major axes are between 6,500 <math>a</math> <math>< 7,000</math> km. The new population has 87 objects with the semi-major axes within that range. The new synthetic cloud of FENGYUN 1C has 174 pieces of space debris whose semi-major axes are within that range. We repeat the process for all the different ranges according to Table 1. We proceed in a similar way for the remaining components of the attribute vector, and consequently, we have a synthetic population of space debris compound of  $2n$  pieces of space debris.

Figure 3 shows the initial distribution of the pieces that compound the cloud of space debris of FENGYUN 1C (data taken from TLE catalog on December 3, 2014). We observe the same distribution as the one obtained by Pardini et al. (2007).<sup>13</sup> Following the previous technique, we generate a new cloud of space debris compound of double elements, and we illustrate the new cloud of space debris in Figure 4, which includes the objects that are in Figure 3 plus the new ones. We observe a similar distribution in both cases.

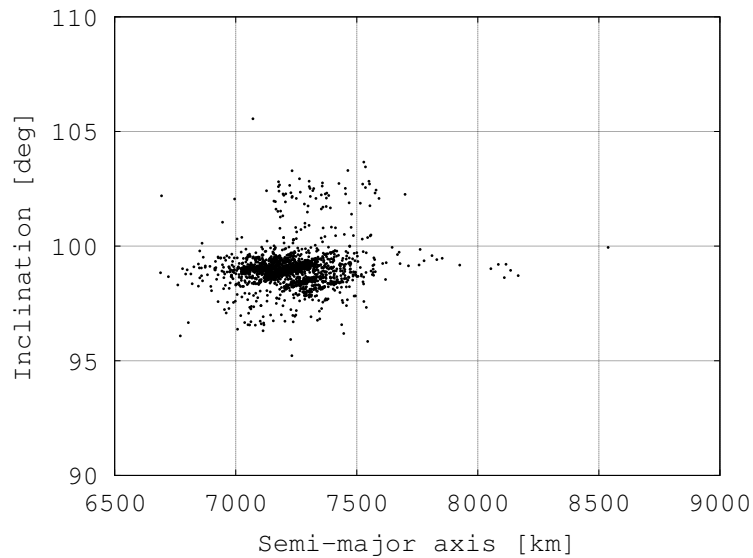


**Figure 3. Distribution of the space debris of the cloud of FENGYUN 1C**

Thanks to NIMASTEP, it is possible to propagate during 10 years both clouds of space debris and observe the differences between them. In particular, Figure 5 and Figure 6 show the distribution of the pieces that compound the FENGYUN 1C cloud of space debris, and the synthetic cloud of space debris (with double elements) after ten years, respectively.

The two clouds basically maintain the same distribution in altitude and inclination. Furthermore, the global predictions that can be extrapolated from the synthetic population are similar as the ones from the real one. In conclusion, a synthetic population, which is compound of real data and artificial data, gives enough information without knowing all the elements of the cloud.



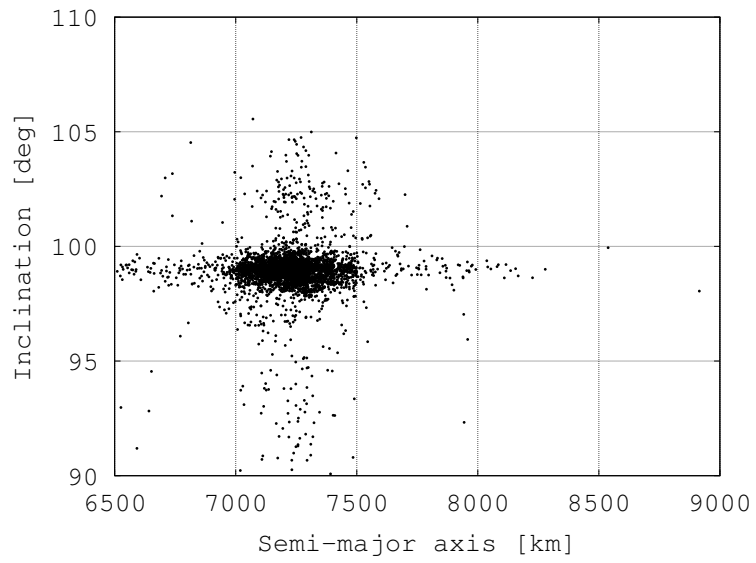


**Figure 4. Distribution of the space debris of the synthetic cloud of FENGYUN 1C**

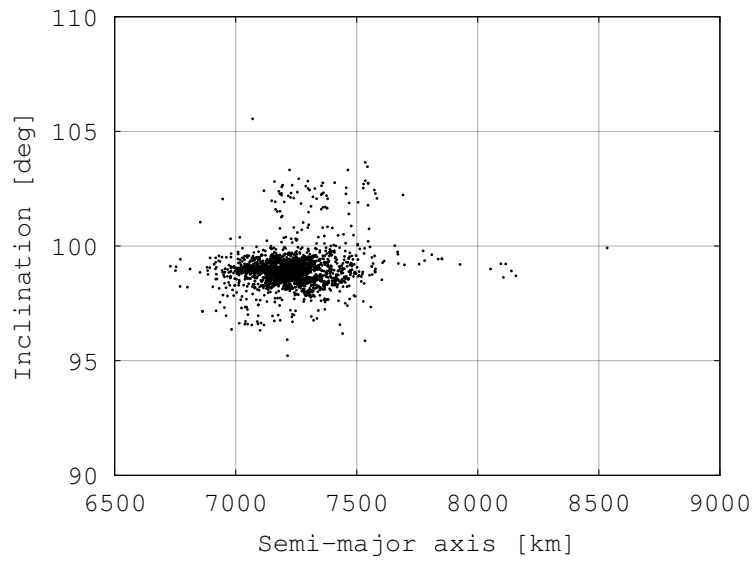


**Figure 5. Distribution of the space debris of the cloud of FENGYUN 1C after 10 years.**

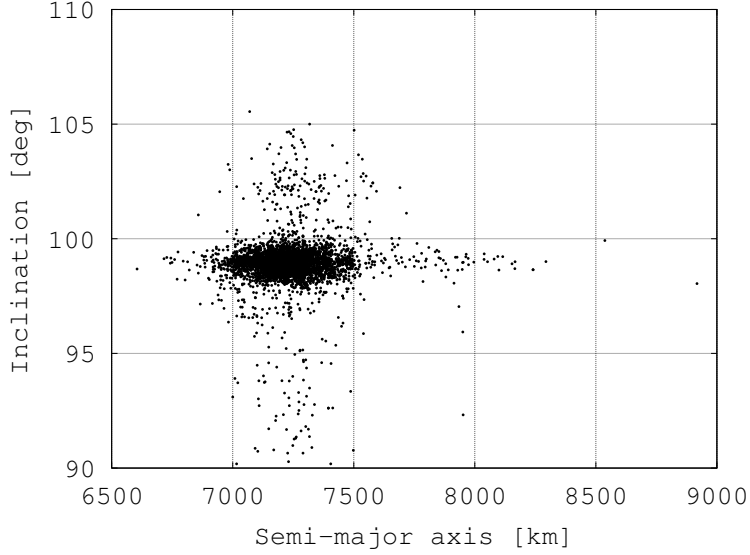


**Figure 6. Distribution of the space debris of the synthetic cloud of FENGYUN 1C after 10 years (first technique)**

### Synthetic Population Created by the Second Technique

We consider the same initial cloud of space debris as in the previous section, meaning that the marginal distribution of each element of the attribute vector will be as in the previous example. Then, we have a similar synthetic population with a particular difference, the computation of the BSTAR coefficient follows a different procedure.

As we illustrate in Figure 2 most of the elements that compound the cloud of FENGYUN 1C have a BSTAR coefficient smaller than 0.005. As we mentioned before, this factor is related with the area-to-mass ratio, meaning that the space debris considered is expected to have a small  $A/m$  ratio. The second technique that we use to generate the new elements of the synthetic population is based on considering a high  $A/m$  ratio since we think that the real population of space debris has hundreds of non-cataloged objects with a big  $A/m$  ratio, which translates into a big BSTAR coefficient.

We consider that the new objects of the population have a bigger BSTAR coefficient. The idea is to invert the data obtained from the initial population given in Table 2. Then, the new  $n$  objects of the synthetic population will have a BSTAR coefficient according to the Table 3.

**Table 3. Frequencies of the BSTAR coefficient for the synthetic cloud of FENGYUN 1C**

BSTAR [ $r_{\oplus}-1$ ]	Objects	BSTAR [ $r_{\oplus}-1$ ]	Objects
$\beta^* < 0.0$	251	$0.0 < \beta^* < 0.0005$	293
$0.0005 < \beta^* < 0.001$	395	$0.001 < \beta^* < 0.0015$	463
$0.0015 < \beta^* < 0.002$	9	$0.002 < \beta^* < 0.003$	48
$0.003 < \beta^* < 0.004$	214	$0.004 < \beta^* < 0.005$	148
$0.005 < \beta^* < 0.01$	317	$\beta^* > 0.01$	515

In this case it is also possible to compare the initial distribution of the pieces of space debris of the FENGYUN 1C population, and the synthetic population. The distribution will be exactly the

same as in the previous subsection. However, in this second technique, it is interesting to show the difference in the BSTAR coefficient in the two clouds of space debris. In Figure 7 and Figure 8 we illustrate the semi-major axis versus the BSTAR coefficient for the FENGYUN 1C population and the synthetic one, respectively. We observe that the number of objects with bigger BSTAR coefficient (higher  $A/m$  ratio) are substantially increased in the synthetic population.

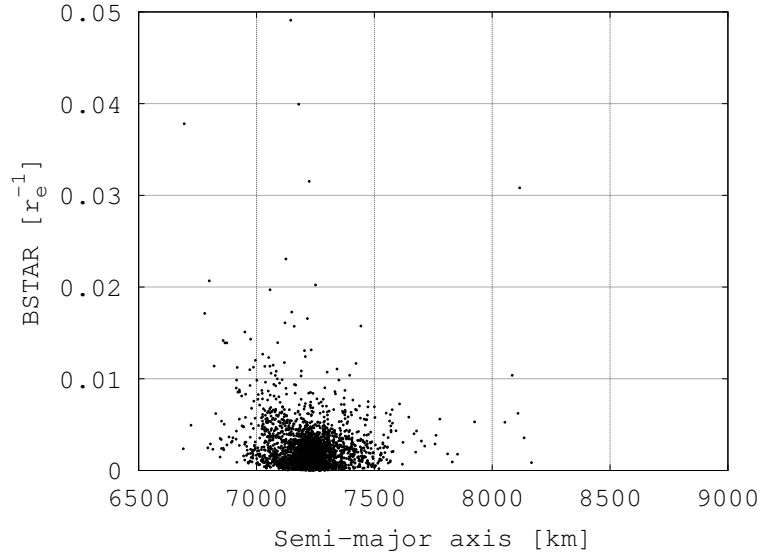


**Figure 7. BSTAR coefficient of the cloud FENGYUN 1C**

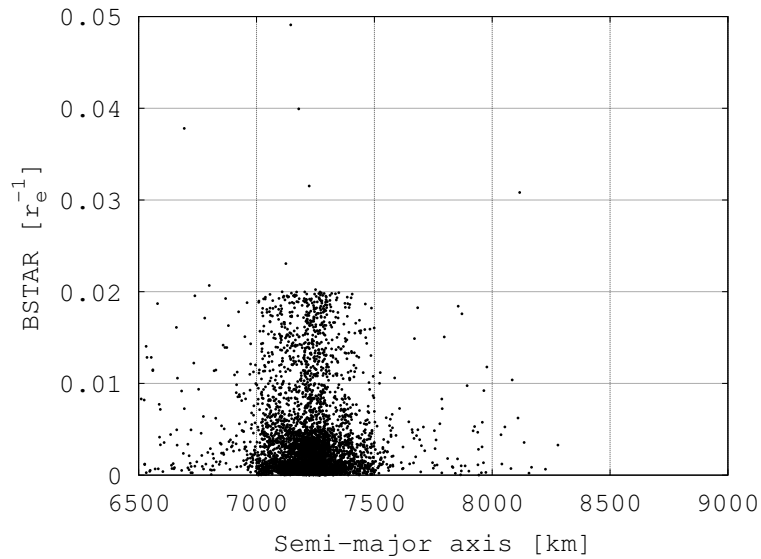


**Figure 8. BSTAR coefficient of the synthetic cloud of FENGYUN 1C**

Thanks to NIMASTEP it is also possible to analyze the evolution of the FENGYUN 1C cloud of space debris and the synthetic one during 10 years.

Figure 9 illustrates the semi-major axis versus the inclination of the synthetic population, where

the new elements of the cloud have a completely different BSTAR coefficient. It is possible to compare with the synthetic population that we obtained by using the technique 1, illustrated in Figure 6, where the new objects have a similar BSTAR coefficient.

In this particular case, the two clouds basically maintain the same distribution in altitude and inclination, making our variation of the BSTAR coefficient meaningless for a ten years propagation. It is expected a different distribution between the two clouds after 10 years propagation when the BSTAR coefficient is much bigger than in our second technique.

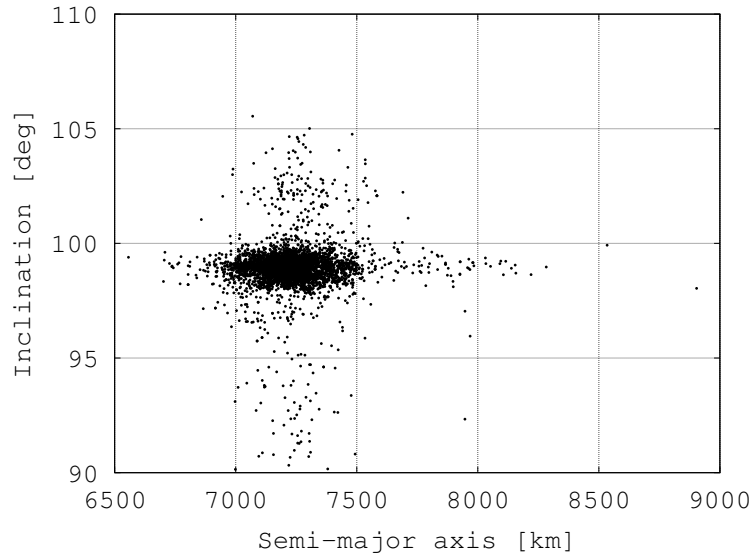


**Figure 9. Distribution of the space debris of the synthetic cloud of FENGYUN 1C after 10 years (second technique)**

## CONCLUSION

Space debris have increased substantially in the last decades. For that reason, this paper introduce the idea of the necessity of a synthetic population of space debris, where millions of pieces of non-cataloged space debris objects can be included. As a first approach we propose two different techniques to include non-cataloged objects to the FENGYUN 1C cloud of space debris. Both techniques result into a synthetic population which have similar properties as the real one. Thanks to the powerful integrator NIMASTEP, it is possible to obtain precisely the orbital position of each piece of space debris that compound the synthetic cloud in a reasonable time due to the parallelization techniques that have been developed.

As a future work it is necessary a rigorous analysis of the influence of the BSTAR coefficient to the different objects of the cloud of space debris, since in lower orbits the atmospheric drag plays a crucial role for the decay of the space debris objects, making the BSTAR coefficient ( $A/m$  ratio) a crucial variable.

The final idea consists of creating a synthetic population of space debris, where the cataloged objects are included in addition to the artificial ones. The synthetic population will give global predictions of the space debris population.

## ACKNOWLEDGMENT

The work of D. Casanova was supported by the research project with reference CUD1315 in the organism Centro Universitario de la Defensa de Zaragoza, and by the Spanish Ministry of Economy and Competitiveness (Project no. ESP201344217-R). The work of A. Petit was supported by a FRIA PhD grant in the Department of Mathematics at the University of Namur.

## REFERENCES

- [1] J. Barthelemy and P. Toint, “Synthetic population generation without a sample,” *Transportation Science*, Vol. 47, No. 2, 2013, pp. 266–279.
- [2] C. Cirillo, E. Cornelis, and P. Toint, “A model of weekly labor participation for a belgian synthetic population,” *Networks and Spatial Economics*, Vol. 1, 2010, pp. 59–73.
- [3] C. Pardini and L. Anselmo, “Physical properties and long-term evolution of the debris clouds produced by two catastrophic collisions in Earth orbit,” *Advances in Space Research*, Vol. 48, No. 3, 2011, pp. 557–569.
- [4] W. Deming and F. Stephan, “A least squares adjustment of a sampled frequency table when the expected marginal totals are known,” *Annals of Mathematical Statistics*, Vol. 11, 1940, pp. 428–444.
- [5] N. Delsate and A. Compère, “NIMASTEP: a software to modelize, study, and analyze the dynamics of various small objects orbiting specific bodies,” *Astronomy and Astrophysics*, Vol. 540, 2012, p. 120.
- [6] C. Hubaux, A.-S. Libert, N. Delsate, and T. Carletti, “Influence of Earths shadowing effects on space debris stability,” *Advances in Space Research*, Vol. 51, No. 1, 2013, pp. 25–38.
- [7] D. Casanova and A. Lemaitre, “Long-term evolution of space debris under the  $J_2$  effect and solar radiation pressure,” *Celestial Mechanics and Dynamical Astronomy*, 2014 (Submitted).
- [8] D. Casanova and A. Lemaitre, “Influence of the area-to-mass ratio on the long-term evolution of space debris in the quasi-GEO region,” *Advances in Space Research*, 2014 (Submitted).
- [9] B. R. Bowman, W. Kent Tobiska, F. A. Marcos, and C. Valladares, “The JB2006 empirical thermospheric density model,” *Journal of Atmospheric and Solar-Terrestrial Physics*, Vol. 70, No. 5, 2008, pp. 774–793.
- [10] D. Casanova, C. Tardioli, and A. Lemaître, “Space debris collision avoidance using a three-filter sequence,” *Monthly Notices of the Royal Astronomical Society*, Vol. 442, No. 4, 2014, pp. 3235–3242.
- [11] D. Casanova, C. Tardioli, and A. Lemaître, “New methods for space debris collision assessment,” *Proceedings IAU Symposium No. 310*, 2014.
- [12] R. J. Beckman, K. A. Baggerly, and M. D. McKay, “Creating synthetic baseline populations,” *Transportation Research Part A: Policy and Practice*, Vol. 30, No. 6, 1996, pp. 415–429.
- [13] C. Pardini and L. Anselmo, “Evolution of the debris cloud generated by the Fengyun-1C fragmentation event,” *NASA Space Flight Dynamics Symposium*, 2007.